Titanium $\alpha - \omega$ phase transformation pathway and a predicted metastable structure

Article · October 2015

DOI: 10.1103/PhysRevB.93.020104 · Source: arXiv

2 authors:

Nikolai Zarkevich
U.S. Department of Energy
47 PUBLICATIONS **474** CITATIONS
SEE PROFILE

Duane D. Johnson
Iowa State University
352 PUBLICATIONS **5,789** CITATIONS
SEE PROFILE

Titanium $\alpha - \omega$ phase transformation pathway and a predicted metastable structure

N. A. Zarkevich,[1] and D. D. Johnson[1,2*]
[1] *The Ames Laboratory, U.S. Department of Energy, Ames, Iowa 50011-3020 USA; and*
[2] *Materials Science & Engineering, Iowa State University, Ames, Iowa 50011-2300 USA.*

As titanium is a highly utilized metal for structural light-weighting, its phases, transformation pathways (transition states), and structures have scientific and industrial importance. Impurities, pressure, and temperature control the phase stability and transition barriers in most industrial and geophysical materials – in Ti, interstitial O, N, or C retard while substitutional Al and V suppress the ω phase. Using a proper solid-state nudged elastic band (SS-NEB) method employing double-climbing images (C2-NEB) combined with density-function theory (DFT+U) methods for accurate energetics, we detail the pressure-induced α (ductile) to ω (brittle) transformation at the coexistence pressure. We find two transition states along the minimal-enthalpy path (MEP) and discover a metastable body-centered orthorhombic (bco) structure, with stable phonons, a lower density than the endpoint phases, and decreasing stability with increasing pressure.

PACS numbers: 64.70.K-, 81.05.Bx, 61.66.Bi, 05.70.Fh

I. INTRODUCTION

Titanium is one of the four (Fe, Cu, Al, Ti) most used structural metals and is the key component of strong, lightweight structural alloys used in aerospace, military, and automotive applications. Mapping competing phases and the associated phase transformations with stress (or pressure, P), temperature (T), and impurities can provide predictive design for improved control of alloy properties, including stabilizing metastable transition structures. For Ti at hydrostatic pressures above 2 GPa, the groundstate hexagonal close-packed (hcp) α-phase can transform into a brittle higher-density ω-phase[1–3] (Fig. 1). At high P, Ti transforms to denser phases: $\alpha \to \omega \to \gamma \to \delta$[4,5], while at high T it transforms to the body-centered cubic (bcc) β-phase[6,7].

Previous theoretical investigations explored the transformation pathway – competing structures, minimum enthalpy pathway (MEP) and transition states (TS) – and some key results are in conflict with observations. For example, from experimental data[1–6,8–15], the $\alpha - \omega$ coexistence P_0 is 2 GPa determined from the inequality $P_{\omega\to\alpha} < P_0 < P_{\alpha\to\omega}$[16], valid for transformations between two solid anisotropic phases. At room temperature, the $\alpha \to \omega$ transition is observed from 2-15 GPa, depending on the pressure environment and sample purity. The $\omega \to \alpha$ transformation is observed below 2 GPa[9], but not for $P \geq 0$ for pure hydrostatic case with a gas, methanol-ethanol, or argon medium[11]. Deviatoric anisotropic (uniaxial or shear) stress narrows the hysteresis[9,11]. The recent theoretical P_0 of 5.7 GPa[17] disagrees with experiment[9]. In addition, Ti has strongly correlated d-electrons, and DFT returns inaccurate relative enthalpies of the groundstate and competing structures (e.g., hcp is not the lowest-energy structure at 0 GPa), with a calculated $P_0 < 0$ between $\alpha - \omega$ phases[18,19], which contradicts the experiments[1–15].

Here we revisit the pressure-induced Ti $\alpha - \omega$ transformation at the coexistence pressure. To detail the MEP and TS, we use the generalized solid-state nudged elastic band (SS-NEB) method[20] based on DFT+U with on-site Hubbard corrections[21] to support the required accurate relative structural enthalpies, atomic forces, and stress tensor for unit cells used for SS-NEB[20]. Importantly, the SS-NEB method properly couples all atomic (or, using periodic unit cells, cell plus internal atomic) degrees of freedom and is mechanically consistent, including the MEP being invariant of cell size[20]. Adjusting $(U - J)$ to 2.2 eV in DFT+U, we correct the inaccurate relative enthalpies and obtain the observed hcp groundstate at 0 GPa, and the observed coexistence pressure $P_0 = 2$ GPa; it is a value that reproduces the observed energy of reduction of Ti oxides (TiO_2 to Ti_2O_3), where 125 kJ/mol was matched by $(U - J) = 2.3 \pm 0.1$ eV[22].

Using SS-NEB combined with DFT+U, we find that the $\alpha - \omega$ transformation has two TS with a local enthalpy minimum, and discover a lower-density, body-centered orthorhombic (bco) metastable structure between them. This $\alpha \to$ bco $\to \omega$ transformation can be considered as a sequence of two transformations. The lower-density, bco metastable TS structure might be stabilized by impurities or negative stresses – potentially induced by chemical interstitial or substitutional alloying.

II. METHODS

We apply the SS-NEB method[20] to detail the MEP (minimum $H = E + PV$) and TS at coexistence pressure P_0. The $\alpha - \omega$ transformation is considered in

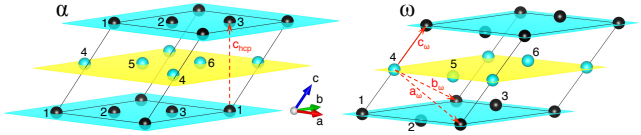

FIG. 1: Enumerated 6-atom unit cells of α (hcp) and ω structures, suitable for the TAO-1 $\alpha - \omega$ transformation[18].

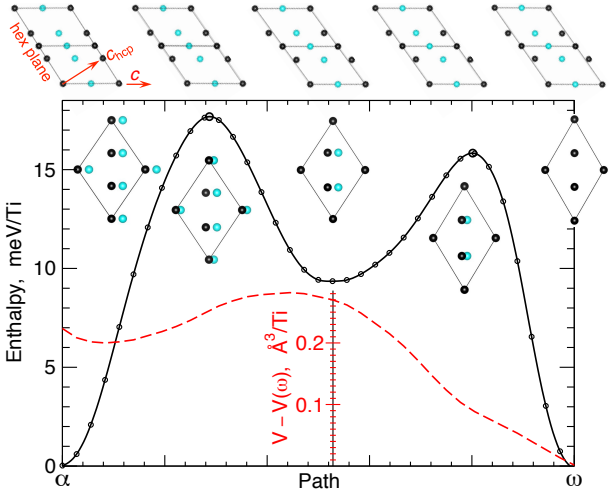

FIG. 2: Enthalpy (meV/atom) versus MEP at $P_0 = 2$ GPa, where α and ω enthalpies are equal within 0.15 meV/Ti. Dashed (red) line is volume V (Å^3/atom) relative to ω (central scale), where V(ω) is 17.55 Å^3/Ti. Atomic motion within 6-atom cell is shown for hcp c-axis (top): dark (black) circles and light (blue) circles indicate two hcp sub-lattices.

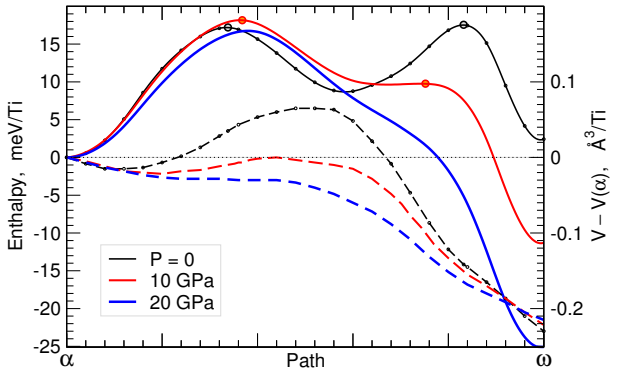

FIG. 3: From SS-NEB (lines) and C2NEB (filled symbols), enthalpy (meV/atom) versus MEP at $P = 0$, 10, and 20 GPa. Change of volume (Å^3 per atom) relative to the α-phase is given by dashed lines (right scale).

a 6-atom unit cell (Fig. 1). For accuracy, we use the C2NEB method[23,24] to verify each TS along the MEP, as tested on shape-memory transforms[25,26]. First, we turn off the climbing and sample the path by equidistant images. Next, one by one, each enthalpy maximum along the path is addressed by C2NEB. We fully relax each local enthalpy minimum and verify its stability.

We employ DFT+U with onsite Hubbard corrections[21] as implemented in VASP,[27,28] based on projector augmented waves (PAW)[29,30] and PW91 exchange-correlation functional.[31] For the 6-atom unit cell (Fig. 1), we use 12^3 k-point mesh in the Brillouin zone, with a denser mesh of 24^3 k-points for the electronic density of states (DOS). Gaussian smearing with $\sigma = 0.05$ eV is used for relaxations; the tetrahedron method with Blöchl corrections[32] is used for the final total-energy calculations. Atomic structures and data[33] are visualized using VESTA[34] and Grace software[35].

Phonons for the predicted bco structure are stable; they are calculated using the small-displacement method as implemented in the Phon code[36]. Results and details are provided in the Supplemental Material.

III. RESULTS

Several mechanisms for the Ti $\alpha - \omega$ transformation have been suggested[1–3,15,18]. In contrast to the previous DFT results for MEP,[18,19] we find hcp Ti (α-phase) to be the stable groundstate at 0 GPa. In Figure 2, from SS-NEB and C2NEB calculations, we report the Ti $\alpha - \omega$ MEP at coexistence $P_0 = 2$ GPa, and MEP versus pressure in Figure 3. Clearly, we find two TS, and, in between, we find a metastable intermediate structure (m), which is body-centered orthorhombic (bco). Hence, the $\alpha - \omega$ MEP consists of $\alpha - m$ and $m - \omega$ transformations, with two barriers along the $\alpha - m - \omega$ path (18 meV and 16 meV, respectively). Recall that each nudged image in the SS-NEB attempts to be equidistant from its neighbors along the MEP, and minimizes its enthalpy in all other directions within the NEB code[20,23,37]. Hence, an enthalpy minimum along the MEP must be a local enthalpy minimum, i.e., a stable or metastable structure. Indeed, being fully relaxed, the local enthalpy minimum m (Fig. 4) does not transform to another structure, and, as expected, it has a stable phonon spectrum (see Supplement). At low pressures, this bco structure has a lower density than the α-phase, see volume in Figs. 2 and 3, and might be stabilized by negative stress or dopants (substitutional or interstitial).

Nonetheless, while a new metastable bco structure is found, the MEP is still the TAO-1 path discussed by Trinkle et al.[18] Other paths, including the α-bcc-ω, suggested by Usikov[2] and ruled out by later experiments,[11]

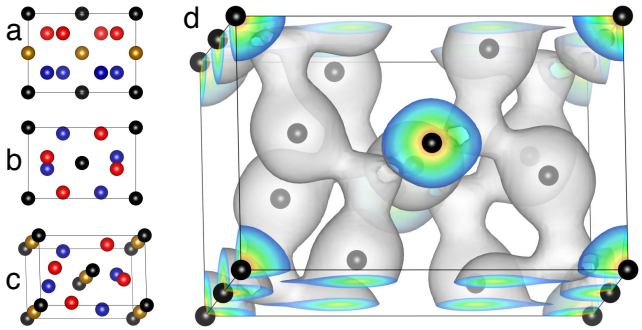

FIG. 4: 12-atom (conventional) unit cell of the metastable bco structure with layers of atoms (left), projected along a (a), b (b), and c (c), where $a < b < c$. (d) iso-surfaces of electronic density (0.033 e^-/Å^3).

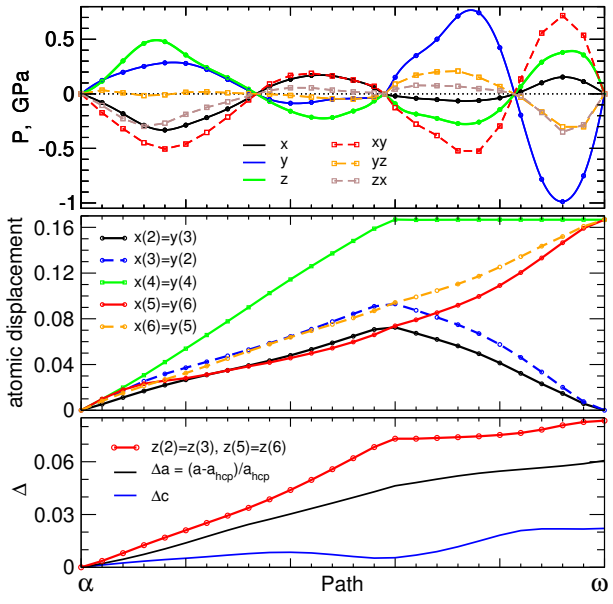

FIG. 5: Diagonal P_i and off-diagonal P_{ij} stress components (GPa), absolute values of the atomic displacements (x, y, z) in direct lattice coordinates (dimensionless), with atom 1 fixed at $(0, 0, 0)$, and elongation Δ (dimensionless) of the lattice translation vectors a and c (relative to the hcp α-phase) in the 6-atom cell (Fig. 1 and Fig. 2 insets) versus MEP at zero pressure.

have substantially higher enthalpy barriers, in agreement with the previous calculations.[18]

At each pressure, we find two barriers in *energy* E for the $\alpha - \omega$ transformation. However, due to volume decrease along the MEP, the second barrier in *enthalpy* $H = E - PV$ is suppressed at $P > 10$ GPa, see Fig. 3, so the stability of the bco structure decreases with pressure. In principle, this metastable intermediate structure during the $\alpha - \omega$ transformation can be determined experimentally by x-ray diffraction (XRD), as this process might be too fast for neutron scattering.

Note that the transformation generates significant anisotropic stress (Fig. 5). On the other hand, pressure anisotropy can facilitate the transformation. Indeed, an applied uniaxial or shear stress narrows the hysteresis in experiment.[9,11] In fact, the reverse $\omega \to \alpha$ transformation does not happen at $P \geq 0$ under hydrostatic conditions. As expected, anisotropic stress disappears at every equilibrium point, either stable (α, m, and ω structures) or unstable (both TS), see Fig. 5. During the whole transformation at P_0, the electronic density of states (DOS) has a minimum near the Fermi energy, E_F for α, m, and ω structures (Fig. 6), as well as both TS configurations, which are the saddle points on the potential enthalpy hypersurface.

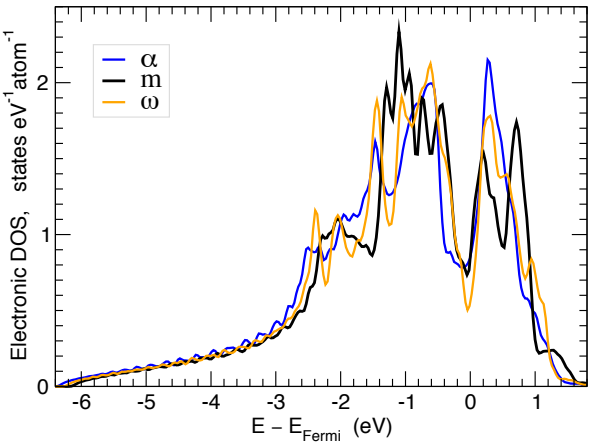

FIG. 6: Electronic DOS versus $E - E_F$ for Ti α, bco, and ω structures at 2 GPa, exhibiting a local minimum at the E_F.

IV. SUMMARY

We have detailed the pressure-induced Ti $\alpha - \omega$ transformation at the coexistence pressure via combined DFT+U[21] and SS-NEB methods[20,23], using two climbing images in C2NEB[23] for multiple transition states. Importantly, DFT+U provides the correct groundstate (α at $P < 2$ GPa), correct relative structural enthalpies, and the observed coexistence pressure P_0 of 2 GPa. Between two transition states (enthalpy barriers) along the minimal-enthalpy path, we discovered a metastable body-centered orthorhombic (bco) structure. The predicted structure has stable phonons and a lower density than the α and ω endpoint phases, but it has decreasing stability with increasing pressure (it is not stable above 10 GPa); it might be stabilized by impurities (under investigation), and provide an opportunity for engineering of lower-density titanium alloys, with additional strengthening by precipitation.

* Electronic address: zarkev@ameslab.gov;ddj@ameslab.gov

[1] J. M. Silcock, Acta Metall. **6**, 481 (1958).
[2] M. P. Uslkov and V. A. Zilbershtein, Phys. Stat. Sol. (a) **19**, 53 (1973).
[3] A. Rabinkln, M. Tallanker and O. Botstein, Acta Metall. **29**, 691 (1981).
[4] Y. K. Vohra and P. T. Spencer, Phys. Rev. Lett. **86**, 3068 (2001).
[5] Y. Akahama, H. Kawamura, and T. Le Bihan, Phys. Rev. Lett. **87**, 275503 (2001).
[6] A. Jayaraman, W. Klement, and G. C. Kennedy, Phys. Rev. **131**, 644 (1963).
[7] J. C. Jamieson, Science **140**, 72 (1963).

[8] V.A. Zilbershteyn, G.I. Nosova, E.I. Estrin, Fiz. Met. Metalloved. **35**, 584 (1973).

[9] V.A. Zilbershteyn, N.P. Chistotina, A.A. Zharov, N.S. Grishina, E.I. Estrin, Fiz. Met. Metalloved. **39**, 445 (1975).

[10] E.Yu. Tonkov, *High Pressure Phase transformations: A Handbook*, vol. 2 (Gordon and Breach Science, Philadelphia, 1992).

[11] D. Errandonea, Y. Meng, M. Somayazulu, and D. Häusermann, Physica B: Condensed Matter **355**, 116 (2005).

[12] Y. Vohra, S. Sikka, S. Vaidya, and R. Chidambaram, Journal of Physics and Chemistry of Solids **38**, 1293 (1977), ISSN 0022-3697.

[13] L.C. Ming, M. Manghnani, M. Katahara, Acta Metall. **29**, 479 (1981).

[14] C.W. Greeff, D.R. Trinkle, R.C. Albers, J. Appl. Phys. **90**, 2221 (2001).

[15] N. Adachi, Y. Todaka, H. Suzuki, and M. Umemoto, Scripta Materialia **98**, 1 (2015), ISSN 1359-6462.

[16] N. A. Zarkevich and D. D. Johnson, Physical Review B **91**, 174104 (2015).

[17] J. Zhang, Y. Zhao, R. S. Hixson, G. T. G. III, L. Wang, W. Utsumi, S. Hiroyuki, and H. Takanori, Journal of Physics and Chemistry of Solids **69**, 2559 (2008), ISSN 0022-3697.

[18] D. R. Trinkle, R. G. Hennig, S. G. Srinivasan, D. M. Hatch, M. D. Jones, H. T. Stokes, R. C. Albers, and J. W. Wilkins, Phys. Rev. Lett. **91**, 025701 (2003).

[19] R. G. Hennig, D. R. Trinkle, J. Bouchet, S. G. Srinivasan, R. C. Albers, and J. W. Wilkins, Nat. Mater. **4**, 129 (2005).

[20] D. Sheppard, P. H. Xiao, W. Chemelewski, D. D. Johnson, and G. Henkelman, J. Chem. Phys. **136**, 074103 (2012).

[21] S.L. Dudarev, G. A. Botton, S.Y. Savrasov, C.J. Humphreys and A.P. Sutton, Phys. Rev. B **57**, 1505 (1998).

[22] S. Lutfalla, V. Shapovalov, and A. T. Bell, Journal of Chemical Theory and Computation **7**, 2218 (2011).

[23] N. A. Zarkevich and D. D. Johnson, J. Chem. Phys. **142**, 024106 (2015).

[24] N. A. Zarkevich and D. D. Johnson, *C2NEB source code*, `http://lib.dr.iastate.edu/ameslab_software/1/` (2014).

[25] N. A. Zarkevich and D. D. Johnson, Phys. Rev. Lett. **113**, 265701 (2014).

[26] N. A. Zarkevich and D. D. Johnson, Phys. Rev. B **90**, 060102 (2014).

[27] G. Kresse and J. Hafner, Phys. Rev. B **47**, RC558 (1993).

[28] G. Kresse, and J. Hafner, Phys. Rev. B **49**, 14251 (1994).

[29] P. E. Blöchl, Phys. Rev. B **50**, 17953 (1994).

[30] G. Kresse, and J. Joubert, Phys. Rev. B **59**, 1758 (1999).

[31] J. Perdew, J. Chevary, S. Vosko, K. Jackson, M. Pederson, D. Singh, and C. Fiolhais, Phys. Rev. B **46**, 6671 (1992), ERRATUM: ibid **48**, 4978 (1993).

[32] P. E. Blöchl, Phys. Rev. B **62**, 6158 (2000).

[33] N. A. Zarkevich, Complexity **11**, 36 (2006).

[34] K. Momma and F. Izumi, J. Appl. Crystallogr. **44**, 1272 (2011).

[35] E. Stambulchik, Grace Development Team, *Grace software*, `http://plasma-gate.weizmann.ac.il/Grace/` (2014).

[36] D. Alfè, Computer Physics Communications **180**, 2622 (2009).

[37] H. Jonsson, G. Mills and K. W. Jacobsen, *Nudged Elastic Band Method for Finding Minimum Energy Paths of Transitions* (World Scientific, 1998).